



## Single-core magnetic markers in rotating magnetic field based homogeneous bioassays and the law of mass action

Jan Dieckhoff<sup>a,\*</sup>, Stefan Schrittwieser<sup>b</sup>, Joerg Schotter<sup>b</sup>, Hilke Remmer<sup>a</sup>, Meinhard Schilling<sup>a</sup>, Frank Ludwig<sup>a</sup>

<sup>a</sup> Institut fuer Elektrische Messtechnik und Grundlagen der Elektrotechnik, TU Braunschweig, Braunschweig, Germany

<sup>b</sup> Molecular Diagnostics, AIT Austrian Institute of Technology, Vienna, Austria



### ARTICLE INFO

#### Article history:

Received 30 June 2014

Received in revised form

14 October 2014

Available online 23 October 2014

#### Keywords:

Magnetic nanoparticle

Rotating magnetic field

Homogeneous bioassay

Binding affinity

### ABSTRACT

In this work, we report on the effect of the magnetic nanoparticle (MNP) concentration on the quantitative detection of proteins in solution with a rotating magnetic field (RMF) based homogeneous bioassay. Here, the phase lag between 30 nm iron oxide single-core particles and the RMF is analyzed with a fluxgate-based measurement system. As a test analyte anti-human IgG is applied which binds to the protein G functionalized MNP shell and causes a change of the phase lag. The measured phase lag changes for a fixed MNP and a varying analyte concentration are modeled with logistic functions. A change of the MNP concentration results in a nonlinear shift of the logistic function with the analyte concentration. This effect results from the law of mass action. Furthermore, the bioassay results are used to determine the association constant of the binding reaction.

© 2014 Elsevier B.V. All rights reserved.

## 1. Introduction

Magnetic nanoparticles (MNP) are well suited as magnetic markers for the realization of bioassay applications. The capability to functionalize the particle surfaces with various biorecognition elements and manipulate them with magnetic fields as well as to measure their magnetic response enables the direct transduction of an analyte binding to an electrical signal. Especially, the so-called homogeneous bioassays or biosensors are promising concepts regarding the increasing need for point-of-care diagnostics [1] because no washing steps are necessary as e.g. for enzyme-linked immunosorbent assays (ELISA) [2]. In contrast to lateral flow techniques [3], these assays offer the possibility to monitor a binding reaction directly in solution. The magnetic excitation of the MNPs in a homogeneous bioassay can be realized with various types of magnetic fields, for instance switched magnetic fields in magnetorelaxometry [4,5] or alternating magnetic fields featuring one or more frequencies [6–9]. In this work, a homogeneous bioassay concept based on rotating magnetic fields (RMF) first presented by Schrittwieser et al. [10] is applied. Compared to an alternating field, the RMF excitation results for Langevin parameters larger than one in a higher measurement effect [11,12], which is the change of the phase lag  $\varphi$  between the rotating

magnetic field and the particle magnetic moments caused by analytes bound to the particle surfaces. For the detection of the single-core magnetic markers, a magnetic detection system is utilized which does not rely on a distinct particle shape [13] or interactions between the particles [14]. Whereas the quantitative detection of a test analyte was practically demonstrated and explained by theory [15], the influence of the particle concentration on the bioassay results was not investigated. Thus, measurement results reflecting the impact of the particle concentration on the phase lag change and the corresponding amount of bound analyte are presented and explained by the law of mass action. Furthermore, the association constant  $K_a$  of the binding reaction is determined and shows a good agreement with literature values.

## 2. Materials and methods

For this bioassay concept, MNPs dominated by the Brownian relaxation process are required. Thus, single-core iron oxide particles with a core diameter  $d_c$  of 30 nm (IPG30) from Ocean NanoTech (Springdale, AR, USA) are used as magnetic markers and the HRP goat anti-Human IgG from ImmunoChemistry Technologies (Bloomington, MN, USA) as a test analyte. Three sample series, each with a fixed MNP concentration of 566 pM, 2.26 nM and 9.06 nM and an increasing IgG concentration, are prepared with a total volume of 150  $\mu$ L in glass vials. The samples are incubated for

\* Corresponding author.

E-mail address: [j.dieckhoff@tu-bs.de](mailto:j.dieckhoff@tu-bs.de) (J. Dieckhoff).

1 h at room temperature to ensure that the binding reaction has reached its equilibrium. For each nanoparticle concentration, one reference sample without IgG exists. In order to investigate the rotational dynamics of magnetic nanoparticles independently of the particle shape and the transparency of the media, a fluxgate-based detection system has been developed [15,16]. This system enables the measurement of the phase lag of the applied MNP down to a particle concentration  $c(\text{MNP})$  of 340 pM or an iron concentration  $c(\text{Fe})$  of 10 µg/ml. The frequency range of the measurements is from 22 Hz to 5 kHz with a field amplitude of 1 mT.

### 3. Theory

#### 3.1. Analyte determination in RMF bioassays

The phase lag of a magnetic nanoparticle ensemble in a rotating magnetic field is expressed by the relation of the imaginary  $M''$  to the real part  $M'$  of its resulting magnetization  $M$  via an arctan function:

$$\varphi = \arctan\left(\frac{M''}{M'}\right) \quad (1)$$

In order to simulate the resulting magnetization, an empirical model derived from a numerical solution of the Fokker–Planck equation [17] is applied as well as a lognormal size distribution for the particle hydrodynamic diameter  $d_h$  and the particle magnetic moment  $m$  with standard deviations  $\sigma_h$  and  $\sigma_m$ .

The increase of the hydrodynamic diameter  $\Delta d_h$  caused by analytes bound to the particle surface is determined by fitting the empirical model to the measured phase lag change curves as a function of the RMF frequency and strength  $\Delta\varphi(f_{\text{RMF}}, H_{\text{RMF}})$ . Here, as a first approximation a direct proportionality was found [15]. Then, the change of the hydrodynamic volume  $\Delta V_h$  is calculated according to

$$\Delta V_h = \frac{\pi}{6}(\Delta d_h)^3 \quad (2)$$

and the amount of bound analyte A per MNP is identified via

$$N_{A,\text{bound}} = \Delta V_h \frac{q_A}{m_A} \quad (3)$$

assuming a constant protein density  $q_A$  of 1.35 g/cm<sup>3</sup> [18] and an average molecular mass  $m_A$  of 270 kDa for the applied test analyte (ImmunoChemistry Technologies). Finally, the absolute concentration of the bound analyte in the solution can be determined via the absolute particle concentration  $c(\text{MNP})$

$$c(A_{\text{bound}}) = c(\text{MNP}) \Delta V_h \frac{q_A}{m_A}. \quad (4)$$

The direct proportionality between the mass and the volume of different proteins in solution was verified by the measurement of the diffusion coefficient by Krouglova et al. [19] and successfully applied by Röcker et al. [20] to describe the relation between the number of proteins adsorbed to a nanoparticle surface and the particle's resulting hydrodynamic growth.

#### 3.2. Law of mass action

A reversible binding reaction between two reactants A and G that form the product AG



can be described at its equilibrium via the law of mass action [21]

$$K_a = \frac{c(AG)}{c(A)c(G)}. \quad (6)$$

$K_a$  represents the association constant, which describes the strength of the affinity in a binding reaction. The reactant concentrations  $c(A)$  and  $c(G)$  are related to the initially applied concentrations  $c_0$  according to

$$c(A) = c_0(A) - c(AG) \quad (7)$$

$$c(G) = c_0(G) - c(AG) \quad (8)$$

If the concentration of the products  $c(AG)$  can be measured and the initial concentrations are known,  $K_a$  can be determined by fitting the measurement results with the following formula derived from Eqs. (6) to (8) [2]:

$$c(AG) = \frac{\left(c_0(G) + c_0(A) + 1/K_a\right) - \left[\left(c_0(G) + c_0(A) + 1/K_a\right)^2 - 4 c_0(G)c_0(A)\right]^{1/2}}{2} \quad (9)$$

Here, it can be seen that the concentration of the products does not scale linearly with the initial concentrations of the reactants. In fact, below the concentration range of the inverse association constant the concentration relation of the products to the initial reactants starts to shrink significantly. Assuming that each MNP is covered with an effective number of biorecognition elements  $N_{\text{cov}}$ , in our case protein G, the initial concentration of the reactant G can be replaced by

$$c_0(G) = N_{\text{cov}} c(\text{MNP}). \quad (10)$$

With  $c_0(A)$  as the initial analyte concentration and  $c(AG) = c(A_{\text{bound}})$  as the concentration of analyte bound to the particles Eq. (9) can be applied to the results of the nanoparticle based bioassay.

### 4. Results and discussion

Fig. 1 shows the phase lag change curves of two samples with a fixed MNP concentration of 2.26 nM and different analyte concentrations of 11.3 nM and 226 nM. Here, the phase lag change  $\Delta\varphi$  denotes the difference in phase lag between a sample with analyte and a reference sample without analyte. Each curve possess a wide

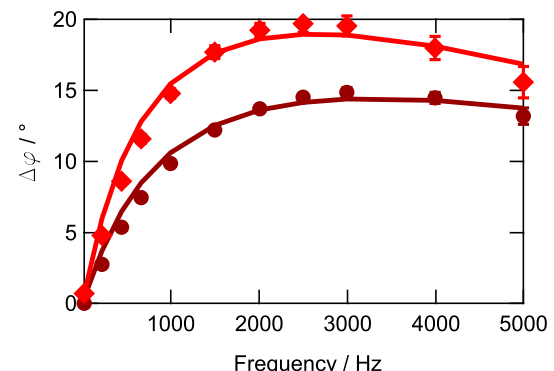


**Fig. 1.** Measured (symbols) and simulated (lines)  $\Delta\varphi$  as a function of  $f_{\text{RMF}}$  for two samples with  $c(\text{MNP}) = 2.26 \text{ nM}$  and  $c_0(A) = 11.3 \text{ nM}$  (circles) as well as  $c_0(A) = 226 \text{ nM}$  (squares). The simulation parameters are  $m(\sigma_m) = 4.4 \text{ aAm}^2 (0.3)$ ,  $d_{h,11.3\text{nM}}(\sigma_h) = 62.5 \text{ nm (0.26)}$ ,  $d_{h,226\text{nM}}(\sigma_h) = 69.5 \text{ nm (0.27)}$ , temperature  $T = 298.5 \text{ K}$  and viscosity  $\eta = 0.88 \text{ mPa s}$ . The error bars represent the standard deviation of five measurements.

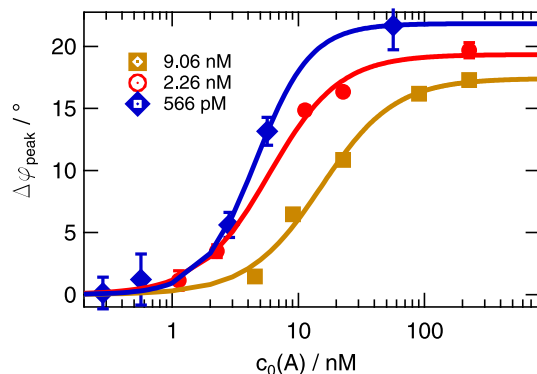


**Fig. 2.** Measured  $\Delta\varphi_{peak}$  (symbols) as a function of  $c_0(A)$  for MNP concentrations of 9.06 nM, 2.26 nM and 566 pM. Lines represent fit with logistic function (11).

spread maximum that lies in the frequency range between 2.5 kHz and 5 kHz for 1 mT. The peak value  $\Delta\varphi_{peak}$  grows for each sample series with increasing analyte concentration. Thus, the bioassay can be calibrated by measuring  $\Delta\varphi_{peak}$  as a function of the analyte concentration for a known sample series and fit the measurement results with a logistic function [15]. This was performed for the three sample series with different particle concentrations and is displayed in Fig. 2. The fit parameters of the logistic function

$$\Delta\varphi_{peak} = B - \frac{B}{1 + \left(\frac{c_0(A)}{c_{0,half}}\right)^{\alpha}} \quad (11)$$

are presented in Table 1.  $B$  displays the maximum value of  $\Delta\varphi_{peak}$  and corresponds to the maximum number of bound analytes. The parameter  $c_{0,half}$  describes the analyte concentration which causes  $\Delta\varphi_{peak} = B/2$  and  $\alpha$  denotes the slope of the curvature.

The curves in Fig. 2 are shifted to lower analyte concentrations with decreasing particle concentration. However, this shift is nonlinear, which is significantly expressed by the fit parameter  $c_{0,half}$ . When the particle concentration is decreased by a factor of 4 from 9.06 nM to 2.26 nM, the parameter  $c_{0,half}$  is only reduced by a factor of 2.6. A further decrease of the particle concentrations by a factor of 4 from 2.26 nM to 566 pM leads to an again smaller reduction of  $c_{0,half}$  by a factor of 1.25. This implies that with a decreasing MNP concentration, a higher concentration of initial analytes per MNP is required to achieve the same coverage of analytes per particle. The law of mass action (see Section 3.2) gives a reasonable explanation for this effect since the particle concentrations reach the range of the inverse association constant for a binding reaction between protein G and IgG [22]. The increase of parameter  $B$  with a decreasing particle concentration is most probably caused by a decreasing concentration of residual buffer solution components that originate from the particle and analyte stock.

In order to determine  $K_a$  and  $N_{cov}$ , the concentration of bound analyte  $c(A_{bound})$  as a function of  $c_0(A)$  is calculated as described in Section 3.1. As can be seen in Fig. 3, the slope of the curves is shifted to higher values of  $c_0(A)$  compared to Fig. 2 because

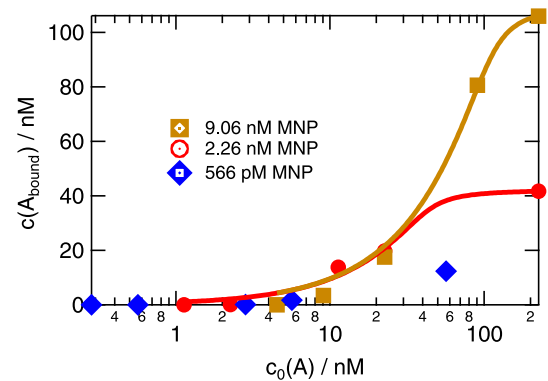


**Fig. 3.** Determined concentration of analyte bound to MNPs as a function of sample analyte concentration for particle concentrations of 9.06 nM, 2.26 nM and 566 pM. Lines represent fits with Eq. (9).

**Table 2**

Fit parameters of  $c(A_{bound})$  as a function of  $c_0(A)$  with Eq. (9) for the three sample series with MNP concentrations of 9.06 nM, 2.26 nM and 566 pM.

$c$ (MNP)	$K_a/M^{-1}$	$N_{cov}$
9.06 nM	$2.39 (\pm 1.76) \cdot 10^8$	$12.12 (\pm 0.69)$
2.26 nM	$5.38 (\pm 4.70) \cdot 10^8$	$18.62 (\pm 1.09)$
566 pM	—	—

$c(A_{bound})$  is, as a first approximation, proportional to  $(\Delta\varphi_{peak})^3$ . Furthermore, the curve with the higher particle concentration possesses the higher rise since here absolute concentrations of the bound analyte are compared. However, the end value of  $c(A_{bound})$  does not scale linearly with the particle concentration. This is a direct consequence of the different  $B$  parameters of the three curves in Fig. 2. The fit of the conversion results with Eq. (9) leads to an approximate determination of  $K_a$  and  $N_{cov}$  (see Table 2) because the number of points in the region of the slope is reduced compared to Fig. 2. For the 566 pM sample series no converging fit could be performed. Nevertheless, the association constants of  $2.39 \times 10^8 \text{ M}^{-1}$  and  $5.38 \times 10^8 \text{ M}^{-1}$  for the sample series with a MNP concentration of 2.26 nM and 9.06 nM lie within the range of the literature values, which are reported in [22] as  $1 \times 10^8 \text{ M}^{-1}$ – $8 \times 10^8 \text{ M}^{-1}$ . The determined  $N_{cov}$  values of 18.62 and 12.12 lie also in a reasonable range taking into account that the manufacturer estimates an average binding of 15 IgG to the MNP protein G shell.

## 5. Conclusions

The impact of the particle concentration on the calibration curves of a homogeneous bioassay based on magnetic nanoparticles in a rotating magnetic field was investigated. A fit of these curves with a logistic function showed that a reduction of the particle concentration did not result in a reduction of the bioassay range by the same factor. This effect is a direct outcome of the law of mass action which describes the relation of two reactant concentrations to the one of the reactants' products. The measured phase lag change curves were converted to the amount of analyte bound to the MNPs. By fitting an equation derived from the law of mass action to the conversion results the association constant  $K_a$  could be determined. This result is an approximate determination due to the reduced number of points in the slope range. However, the values  $2.39 \times 10^8 \text{ M}^{-1}$  and  $5.38 \times 10^8 \text{ M}^{-1}$  for the binding reaction's association constant lie well in the range of the literature values.

**Table 1**

Fit parameters of  $\Delta\varphi_{peak}$  as a function of the sample analyte concentration with a logistic function for MNP concentrations of 9.06 nM, 2.26 nM and 566 pM.

$c$ (MNP)	$B/^\circ$	$c_{0,half}/\text{nM}$	$\alpha$
9.06 nM	$17.42 (\pm 1.05)$	$15.20 (\pm 2.56)$	$1.49 (\pm 0.33)$
2.26 nM	$19.34 (\pm 0.83)$	$5.84 (\pm 0.80)$	$1.56 (\pm 0.20)$
566 pM	$21.84 (\pm 0.7)$	$4.66 (\pm 0.92)$	$1.79 (\pm 0.29)$

## Acknowledgments

This work was supported by the European Commission Framework Programme 7 under the NAMDIATREAM Project (No. NMP-2010-246479).

## References

- [1] P. Yager, G.J. Domingo, J. Gerdes, Point-of-care diagnostics for global health, *Annu. Rev. Biomed. Eng.* 10 (1) (2008) 107–144.
- [2] G. Wu, *Assay Development: Fundamentals and Practices*, Wiley, Hoboken, NJ, 2010.
- [3] N.T.K. Thanh (Ed.), *Magnetic Nanoparticles: From Fabrication to Clinical Applications: Theory to Therapy, Chemistry to Clinic, Bench to Bedside*, CRC Press, Boca Raton, FL, 2012.
- [4] W. Weitschies, R. Kitz, T. Bunte, L. Trahms, Determination of relaxing or remanent nanoparticle magnetization provides a novel binding-specific technique for the evaluation of immunoassays, *Pharm. Pharmacol. Lett.* 7 (1997) 1–4.
- [5] E. Heim, F. Ludwig, M. Schilling, Binding assays with streptavidin-functionalized superparamagnetic nanoparticles and biotinylated analytes using fluxgate magnetorelaxometry, *J. Magn. Magn. Mater.* 321 (10) (2009) 1628–1631.
- [6] J. Connolly, T.G. St Pierre, Proposed biosensors based on time-dependent properties of magnetic fluids, *J. Magn. Magn. Mater.* 225 (1-2) (2001) 156–160.
- [7] S.H. Chung, A. Hoffmann, S.D. Bader, C. Liu, B. Kay, L. Makowski, L. Chen, Biological sensors based on Brownian relaxation of magnetic nanoparticles, *Appl. Phys. Lett.* 85 (14) (2004) 2971.
- [8] C.-Y. Hong, C.C. Wu, Y.C. Chiu, S.Y. Yang, H.E. Horng, H.C. Yang, Magnetic susceptibility reduction method for magnetically labeled immunoassay, *Appl. Phys. Lett.* 88 (21) (2006) 212512.
- [9] L. Tu, Y. Jing, Y. Li, J.-P. Wang, Real-time measurement of Brownian relaxation of magnetic nanoparticles by a mixing-frequency method, *Appl. Phys. Lett.* 98 (21) (2011) 213702.
- [10] S. Schrittweiser, F. Ludwig, J. Dieckhoff, K. Soulantica, G. Viau, L.-M. Lacroix, S. M. Lentijo, R. Boubekri, J. Maynadi, A. Huetten, H. Brueckl, J. Schotter, Modeling and development of a biosensor based on optical relaxation measurements of hybrid nanoparticles, *ACS Nano* 6 (1) (2012) 791–801.
- [11] J. Dieckhoff, T. Yoshida, K. Enpuku, M. Schilling, F. Ludwig, Homogeneous bioassays based on the manipulation of magnetic nanoparticles by rotating and alternating magnetic fields—a comparison, *IEEE Trans. Magn.* 48 (11) (2012) 3792–3795.
- [12] J. Dieckhoff, M. Schilling, F. Ludwig, Magnetic marker based homogeneous bioassays utilizing rotating magnetic fields, *J. Appl. Phys.* 115 (17) (2014) 17B304.
- [13] S. Schrittweiser, F. Ludwig, J. Dieckhoff, A. Tschoepe, A. Guenther, M. Richter, A. Huetten, H. Brueckl, J. Schotter, Direct protein detection in the sample solution by monitoring rotational dynamics of nickel nanorods, *Small* 10 (2) (2014) 407–411.
- [14] A. Ranzoni, G. Sabatte, L.J. van IJzendoorn, M.W.J. Prins, One-step homogeneous magnetic nanoparticle immunoassay for biomarker detection directly in blood plasma, *ACS Nano* 6 (4) (2012) 3134–3141.
- [15] J. Dieckhoff, A. Lak, M. Schilling, F. Ludwig, Protein detection with magnetic nanoparticles in a rotating magnetic field, *J. Appl. Phys.* 115 (2) (2014) 024701.
- [16] J. Dieckhoff, M. Schilling, F. Ludwig, Fluxgate based detection of magnetic nanoparticle dynamics in a rotating magnetic field, *Appl. Phys. Lett.* 99 (11) (2011) 112501.
- [17] T. Yoshida, K. Enpuku, J. Dieckhoff, M. Schilling, F. Ludwig, Magnetic fluid dynamics in a rotating magnetic field, *J. Appl. Phys.* 111 (5) (2012) 053901.
- [18] H. Fischer, I. Polikarpov, A.F. Craievich, Average protein density is a molecular-weight-dependent function, *Protein Sci.* 13 (10) (2009) 2825–2828.
- [19] T. Krouglova, J. Vercammen, Y. Engelborghs, Correct diffusion coefficients of proteins in fluorescence correlation spectroscopy, application to tubulin oligomers induced by mg<sup>2+</sup> and paclitaxel, *Biophys. J.* 87 (4) (2004) 2635–2646.
- [20] C. Röcker, M. Pötzl, F. Zhang, W.J. Parak, A quantitative fluorescence study of protein monolayer formation on colloidal nanoparticles, *Nat. Nanotechnol.* 4 (9) (2009) 577–580.
- [21] R. Reverberi, L. Reverberi, Factors affecting the antigen-antibody reaction, *Blood Transf.* (5) (2007) 227–240.
- [22] K. Saha, F. Bender, E. Gizeli, Comparative study of IgG binding to proteins g and a: nonequilibrium kinetic and binding constant determination with the acoustic waveguide device, *Anal. Chem.* 75 (4) (2003) 835–842.